Mass distributions in monoenergetic-neutron-induced fission of ^{232}Th

L. E. Glendenin, J. E. Gindler, I. Ahmad, D. J. Henderson, and J. W. Meadows
Chemistry Division, Argonne National Laboratory, Argonne, Illinois 60439
(Received 15 February 1980)

Fission product yields for 38 masses were determined for the fission of ^{232}Th with essentially monoenergetic neutrons of 2.0, 3.0, 4.0, 5.9, 6.4, 6.9, 7.6, and 8.0 MeV. Fission product activities were measured by Ge(Li) γ-ray spectrometry of irradiated ^{232}Th foils and by chemical separation of the fission product elements followed by β counting. The mass yield data for ^{232}Th(n,f) show a sensitive increase of fission yields in the near-symmetric mass region (valley) with increasing incident neutron energy E_n and a pronounced dip in yield at the onset of second-chance fission just above the neutron binding energy (at ~ 6 MeV) where the excitation energy is lowered by competition with neutron evaporation prior to fission. The effect of second-chance fission is also seen in the yields of asymmetric peak products. A distinct third peak is observed at symmetry in the valley of the mass distribution, and enhanced yields are observed in the asymmetric peaks at masses associated with even Z (proton pairing effect). The fission yeilds of ^{232}Th(n,f) are compared with those of ^{238}U(n,f) and ^{232}Th(γ,f).

[NUCLEAR REACTIONS, FISSION ^{232}Th(n,f) E_n=2.0, 3.0, 4.0, 5.9, 6.4, 6.9, 7.6, and 8.0 MeV; measured mass yields.]

I. INTRODUCTION

Examination of the literature reveals a lack of data on the characteristics of fission product mass distributions for monoenergetic-neutron-induced fission of ^{232}Th, particularly as a function of incident neutron energy E_n. Ford and Leachman[1] determined the yields of four fission products in the near-symmetric (valley) mass region (^{109}Pd, ^{111}Ag, ^{112}Pd, and ^{113}Ag) at five E_n values in the range of 9.1–18.1 MeV. Dubrovina *et al.*[2] measured the fission yield ratios for seven fission products relative to ^{89}Sr at nine neutron energies between 1.5 and 17.7 MeV. Somewhat more complete mass-yield data obtained for E_n = 3 and 11 MeV are summarized in the compilation by Crouch.[3] Much more extensive data for "fast" reactor neutron fission and for E_n = 14 MeV are given in Ref. 3 and in the compilation by Meek and Rider.[4]

The present work was undertaken to determine in detail the characteristics of the mass distribution for ^{232}Th(n,f) as a function of E_n over the range of 2–8 MeV with particular emphasis on the question of structure in the valley of the mass-yield curve and on the effect of the onset of second-chance fission near E_n = 6 MeV. For this purpose reasonably complete mass distributions (38 masses) were obtained at E_n values of 2.0, 3.0, 4.0, 5.9, 6.4, 6.9, 7.6, and 8.0 MeV.

II. EXPERIMENTAL

A. Neutron irradiations

Targets for the neutron irradiations were 2.54-cm diameter by 0.0254-cm-thick disks of thorium metal with an average weight of 1.3 g. The attenuation of neutrons in the energy range of 2–8 MeV by a target disk was about 0.5%. Irradiations were made at the Argonne Fast Neutron Generator Facility[5] in the manner described by Smith and Meadows.[6] The targets were attached to a low-mass fission chamber containing a thin, standardized deposit of ^{238}U to monitor the fission rate. This assembly was positioned about 3 cm from the neutron source. Neutrons with energies below 5 MeV were produced by the ^{7}Li(p,n)^{7}Be reaction; neutrons of higher energy were produced by the ^{2}H(d,n)^{3}He reaction.

Details of the monoenergetic neutron beam characteristics have been given in a previous publication.[7] Spread in the principal neutron energy ranged from 4–8%. Beam intensities averaged about 3×10^7 cm^{-2} sec^{-1}, and fission rates in a target disk were typically 2×10^4 sec^{-1}. Also present were small contributions to the fission rate by neutrons of other energies arising from the ^{7}Li (p,n)^{7}Be* reaction, from deuteron stripping reactions (primarily in the deuterium target cell), and from elastic and inelastic scattering by the room environment. Small corrections (1 to 8%) were made for the effects of these neutrons on the fission yields of masses that are strongly sensitive to neutron energy (A = 103 to 127). To ensure adequate intensities of fission product activities the targets were irradiated for periods of 14 to 15 h.

B. Fission yield determinations

Fission yields were determined by high-resolution γ-ray spectrometry of an irradiated thorium target or by chemical separation of a fission product element followed by β counting. The two radiometric methods are designated herein as the γ and RC-β methods, respectively. For the measurement of the low intensities of fission product activities in the valley mass region (103 to 127) and for ^{77}As and ^{78}As, it was necessary to employ the more sensitive RC-β method. The γ method was used for all other determinations.

For chemical separation of the fission product elements, the irradiated thorium metal targets were dissolved in concentrated hydrochloric acid containing small quantities of nitric and hydrofluoric acids and carriers for the elements of interest. The elements were then separated, chemically purified, and samples prepared for β counting according to the procedures compiled by Flynn.[8] The samples were counted in a calibrated low-background (0.5 count/min) β proportional counter[8] equipped with an automatic sample changer. The radioactive purity for each sample was verified by following its decay over an extended period of several half-lives. Decay curves were analyzed with the least-squares computer program *CLSQ*.[9] The observed β counting rate at the end of irradiation for each fission product was then corrected for chemical yield, counting efficiency, decay, genetic relationships, and degree of saturation during irradiation to give the saturation activity A_∞.

For γ counting the irradiated targets were mounted on flat stainless steel plates and placed in a computer-controlled sample changer designed to ensure reproducible positioning of samples. The γ-ray spectrometer system was based on an 80-cm^3 lithium-drifted germanium Ge(Li) detector with a resolution of 2.1 keV full width at half maximum (FWHM) for the 1.33-MeV γ-ray of ^{60}Co. Details of this system and the γ counting method are given in a previous publication.[7] To enhance statistical accuracy in the determination of the fission product γ-ray activities, a large number (~40) of γ-ray spectra were recorded over a sufficient period of time (~1 month) to encompass the wide range of half-lives involved. These complex spectra were then analyzed with the computer program GAMANAL[10] to obtain the intensities of the resolved photopeaks.

The fission product γ decay data selected for use in these measurements are presented with references in Table I. Since the largest single source of error in the γ counting method lies in the values taken for absolute γ emission intensities I_γ (listed as photons per 100 disintegrations in Table I), the values were checked by application of the method to thermal-neutron-induced fission of ^{235}U and comparison of the observed fission yields with the

TABLE I. Fission product gamma decay data used in fission yield measurements.

Nuclide	Half-life	E_γ (keV)	I_γ (%)	Ref.
$^{83}Se^g$	22.6 min	356.7	68.6[a]	11
$^{84}Br^g$	31.8 min	881.6	42 ± 4	12
		1897.6	14.9 ± 1.9	12
$^{85}Kr^m$	4.48 h	151.2	75.5 ± 0.6	12
		304.9	14.0 ± 0.5	12
^{87}Kr	76.3 min	402.6	49.5 ± 1.6	12
^{88}Kr	2.84 h	196.3	26.3 ± 1.6	12
		1529.8	11.1 ± 0.7	12
(^{88}Rb)[b]	17.8 min	898.0	14.5 ± 1.0	12
		1836.0	22.1 ± 1.5	12
^{89}Rb	15.2 min	1031.9	59 ± 6	12
		1248.1	43 ± 4	12
^{91}Sr	9.5 h	652.9	11.1 ± 1.0	12
		749.8	23.1 ± 1.2	12
		1024.3	33.5 ± 0.7	12
($^{91}Y^m$)[b]	49.7 min	557.6	60.4 ± 2.1[b]	12
^{92}Sr	2.71 h	1383.9	90 ± 11	12
^{93}Sr	7.3 min	168.5	34.5[a]	11
		590.2	67.7[a]	11
^{93}Y	10.21 h	266.9	6.8 ± 0.4	12
		947.1	1.94 ± 0.11	12
^{94}Y	19 min	919.2	49 ± 2[c]	
^{97}Zr	16.9 h			
($^{97}Nb^m$)[b]	60 sec	743.4	92.8 ± 0.9[b]	12
($^{97}Nb^g$)[b]	72.1 min	657.9	105.9 ± 1.1[b]	12
^{99}Mo	66.0 h	140.5	5.7 ± 0.5	12
		181.1	6.52 ± 0.19	12
		739.5	13.0 ± 0.4	12
($^{99}Tc^m$)[b]	6.02 h	140.5	84.9 ± 0.9[b]	12
^{101}Tc	14.1 min	306.9	88 ± 6	12
^{129}Sb	4.35 h	812.6	43.5[a]	11
^{131}I	8.04 d	364.5	81.2 ± 1.1	12
^{132}Te	78.2 h	228.2	88.2 ± 0.2	12
(^{132}I)[b]	2.30 h	522.7	16.6 ± 0.6[b]	12
		667.7	101.7 ± 0.1[b]	12
		772.6	78.5 ± 1.9[b]	12
^{133}I	20.8 h	529.9	87.3 ± 0.2	12
^{134}Te	41.8 min	180.9	17.9 ± 1.0	12
		278.0	21.2 ± 1.0	12
		566.0	18.8 ± 1.0	12
		742.6	14.7 ± 0.7	12
		767.2	29.9 ± 0.8	12
^{135}I	6.61 h	1038.8	7.9 ± 0.3	12
		1131.5	22.5 ± 0.8	12
		1260.4	28.6 ± 1.0	12
		1457.6	8.6 ± 0.3	12
		1678.0	9.5 ± 0.4	12
		1791.2	7.70 ± 0.25	12
($^{135}Xe^m$)[b]	15.3 min	526.6	14.0 ± 0.5[b]	12
^{138}Xe	14.2 min	258.3	31.5 ± 1.3	12
		1768.3	16.7 ± 0.7	12
^{138}Cs	32.2 min	462.8	30.7 ± 0.7	12
		1009.8	29.8 ± 0.7	12
		1435.9	76.3 ± 1.6	12
^{139}Ba	83.0 min	165.9	22 ± 1[c]	
^{140}Ba	12.79 d	537.3	24[a]	11
(^{140}La)[b]	40.22 h	487.0	49.5 ± 0.2[b]	12
		815.9	25.9 ± 0.8[b]	12
		1596.5	110.0 ± 0.2[b]	12

TABLE I. (*Continued.*)

Nuclide	Half-life	E_γ (keV)	I_γ (%)	Ref.
^{141}Ba	18.2 min	190.2	46 ± 4	12
		277.0	23.3 ± 2.0	12
		304.2	25.2 ± 2.2	12
		343.7	14.2 ± 1.3	12
^{141}Ce	32.5 d	145.4	48.0 ± 2.0	12
^{142}La	92.7 min	641.2	46 ± 2^{c}	
		894.9	9.4 ± 1.2	12
		1901.3	8.7 ± 0.8	12
^{143}Ce	33.0 h	293.3	43.4 ± 2.0	12
^{146}Ce	14.2 min	218.3	21.5^{a}	11
		316.8	55^{a}	11
^{147}Nd	11.06 d	91.1	27.9 ± 0.5	12
		531.0	13.1 ± 0.8	12
^{149}Nd	1.76 h	114.3	18.8 ± 2.0	12
		211.3	27.3 ± 1.8	12

[a]Uncertainty of ±10% assumed.
[b]In equilibrium with parent nuclide.
[c]I_γ from measurement of fission yield in ^{235}U(n,f) (see text).

well-known values given in the compilations of Refs. 3 and 4. With the exceptions of ^{94}Y, ^{139}Ba, and ^{142}La, it was found that the use of I_γ values from Refs. 11 and 12 given in Table I resulted in satisfactory agreement. For ^{94}Y, ^{139}Ba, and ^{142}La, the empirical values of I_γ determined in ^{235}U(n,f) are used in the present work.

The measured fission product γ-ray activities from the GAMANAL[10] program were analyzed by the decay program CLSQ[9] to obtain the activities at the end of irradiation. Further corrections were made as required for counting efficiency, cascade coincidence losses,[7] absolute γ emission intensities (Table I), genetic relationships, and degree of saturation during irradiation to give the saturation activity A_∞.

Values of A_∞ determined by the methods just described are related to fission yields by the expression

$$\text{fission yield} = A_\infty/\text{fission rate}. \tag{1}$$

Since a suitable ^{232}Th monitor for the fission chamber was not available, a ^{238}U monitor was used to provide an approximate fission rate. The fission yields were then placed on an absolute basis by normalization of the complete mass distribution to 200% total yield, the undetermined yields being interpolated or extrapolated from measured yields. As only ~30% of the total yield was undetermined, the uncertainty (1 σ) in the fission rate obtained by the normalization procedure is only 2% when a 20% error is assigned to all interpolated or extrapolated values.

III. RESULTS AND DISCUSSION

The results of the fission product yield determinations are presented in Table II and depicted graphically as mass-yield curves in Fig. 1. Also shown for comparison in Fig. 1 is the mass distribution for $E_n = 14$ MeV based on the average of the fission yield data compiled in Refs. 3 and 4. Uncertainties (1 σ) in the fission yield values were obtained by consideration of all known sources of random and systematic error with the usual rules of error propagation. For fission yields measured by the γ method, σ values fall typically in the range of 3 to 10%. Larger uncertainties ranging from 10 to 25% are associated with the yields measured by the RC-β method. An assessment of possible error in determination of the mass yield due to direct formation in fission (independent yield) of chain members beyond the one measured was made using the charge distribution systematics of Wolfsberg.[13] For the E_n range of 2–8 MeV, calculated cumulative yields for the fission products in Table II are > 99% with the exception of ^{134}Te (92 to 95%). The data in Table II contain no corrections for possible charge distribution effects.

The salient features apparent from the mass distributions shown in Fig. 1 are (1) the strong dependence of fission yields in the valley mass region on E_n (increased probability of near-symmetric fission with increasing excitation energy), (2) the existence of a definite symmetric fission peak (around $A = 115$) in the valley, and (3) the appearance of fine structure, presumably caused by the proton pairing effect,[14] near masses 90, 96, 134, and 140, where yields are enhanced for even atomic numbers $Z = 36$, 38, 52, and 54. Both the symmetric peak and the fine structure appear to "wash out" slowly with increasing E_n.

Since the literature data[3,4] on fast neutron fission of ^{232}Th leave considerable uncertainty as to the existence of a third peak at symmetry in the mass distribution, a special effort was made in the present work to outline carefully the valley region. The results are shown in Fig. 2, where mass yields are plotted for $E_n = 4.0$ and 5.9 MeV. For the isomers ^{115}Cd^{g} and ^{121}Sn^{g}, the total chain yields were obtained by assuming isomer ratios $(m+g)/g$ of 1.11 ± 0.05 for ^{115}Cd^{g} (average value for several fissioning systems in Ref. 4) and 1.16 ± 0.11 for ^{121}Sn^{g} (Ref. 15). The peak at symmetry is clearly apparent and is seen to diminish with the increase of E_n from 4.0 to 5.9 MeV. Data of poorer quality obtained at 2 and 3 MeV are consistent with the curves shown in Fig. 1. The peak is still apparent to a slight extent at $E_n = 14$ MeV (see Fig. 1).

Some mass distribution characteristics derived

TABLE II. Fission product yields in monoenergetic-neutron-induced fission of ^{232}Th.

Fission product	Measurement technique	Incident neutron energy (MeV) 2.0	3.0	4.0	5.9	6.4	6.9	7.6	8.0
^{77}As	RC-β					0.039 ± 0.006		0.029 ± 0.004	
^{78}As	RC-β					0.065 ± 0.010		0.078 ± 0.012	
^{83}Se^m	γ	0.93 ± 0.21	1.12 ± 0.20	0.91 ± 0.15		1.25 ± 0.27	1.44 ± 0.26	1.38 ± 0.22	1.85 ± 0.28
^{84}Br^g	γ	4.54 ± 0.48	4.05 ± 0.52	4.35 ± 0.47	4.02 ± 0.76	5.34 ± 0.65	5.50 ± 0.71	5.05 ± 0.60	5.47 ± 0.53
^{85}Kr^m	γ	5.13 ± 0.21	4.38 ± 0.17	4.17 ± 0.16	4.00 ± 0.20	5.70 ± 0.22	6.82 ± 0.33	6.01 ± 0.26	5.81 ± 0.20
^{87}Kr	γ	7.37 ± 0.34	6.85 ± 0.33	6.21 ± 0.30	5.28 ± 0.30	6.80 ± 0.31	7.61 ± 0.39	7.10 ± 0.35	7.44 ± 0.30
^{88}Kr	γ	6.93 ± 0.29	6.64 ± 0.27	6.16 ± 0.25	5.71 ± 0.27	6.46 ± 0.25	7.55 ± 0.34	7.03 ± 0.30	6.71 ± 0.25
^{89}Rb	γ	7.70 ± 0.64	7.56 ± 0.67	7.18 ± 0.58	7.49 ± 1.00	7.97 ± 0.71	6.98 ± 0.66	7.07 ± 0.64	7.76 ± 0.84
^{91}Sr (Y)	γ	7.82 ± 0.24	7.71 ± 0.23	7.30 ± 0.21	6.63 ± 0.21	6.93 ± 0.16	7.28 ± 0.23	7.15 ± 0.21	7.15 ± 0.20
^{92}Sr	γ	7.24 ± 0.87	7.23 ± 0.88	6.93 ± 0.86	6.56 ± 0.81	6.26 ± 0.76	6.46 ± 0.81	6.45 ± 0.78	6.62 ± 0.81
^{93}Y	γ	5.61 ± 0.38	6.09 ± 0.43	5.68 ± 0.38	4.85 ± 0.49	4.71 ± 0.37	5.21 ± 0.44	5.26 ± 0.38	5.01 ± 0.39
^{94}Y	γ	5.79 ± 0.36	6.07 ± 0.67	6.20 ± 0.35	4.48 ± 1.23	4.75 ± 0.93	4.79 ± 1.16	5.58 ± 0.66	5.19 ± 0.39
^{97}Zr (Nb)	γ	4.50 ± 0.12	4.87 ± 0.15	4.85 ± 0.13	4.80 ± 0.13	3.38 ± 0.11	3.50 ± 0.10	3.62 ± 0.13	3.59 ± 0.10
^{99}Mo (Tc)	γ	2.87 ± 0.17	3.15 ± 0.16	3.41 ± 0.15	3.79 ± 0.23	2.60 ± 0.13	2.09 ± 0.16	2.21 ± 0.13	2.25 ± 0.23
^{101}Tc	γ	0.82 ± 0.15	1.08 ± 0.12	1.25 ± 0.11	1.77 ± 0.22	1.22 ± 0.15	0.78 ± 0.32	1.00 ± 0.12	1.08 ± 0.15
^{103}Ru	RC-β		≤0.15	0.15 ± 0.04	0.67 ± 0.10	0.16 ± 0.04			
^{105}Ru	RC-β		≤0.011	0.037 ± 0.004	0.24 ± 0.05	0.13 ± 0.02	0.18 ± 0.03		
^{109}Pd	RC-β		0.016 ± 0.007	0.036 ± 0.005	0.19 ± 0.03	0.14 ± 0.03	0.13 ± 0.02	0.18 ± 0.04	0.18 ± 0.04
^{111}Ag	RC-β	≤0.004	0.027 ± 0.003	0.076 ± 0.008	0.29 ± 0.03	0.20 ± 0.03	0.17 ± 0.02	0.22 ± 0.03	0.28 ± 0.03
^{112}Pd	RC-β		0.028 ± 0.004	0.097 ± 0.011	0.30 ± 0.04	0.24 ± 0.04	0.18 ± 0.03	0.26 ± 0.04	0.28 ± 0.05
^{115}Cd^g	RC-β	0.005 ± 0.001	0.023 ± 0.004	0.099 ± 0.015	0.27 ± 0.04	0.23 ± 0.04	0.20 ± 0.03	0.20 ± 0.03	0.29 ± 0.04
^{121}Sn^g	RC-β			0.063 ± 0.010	0.19 ± 0.03	0.14 ± 0.03		0.21 ± 0.04	
^{127}Sb	RC-β	0.003 ± 0.001		0.056 ± 0.011	0.22 ± 0.04	0.18 ± 0.03	0.15 ± 0.03	0.20 ± 0.03	0.26 ± 0.05
^{129}Sb	RC-β	0.11 ± 0.02	0.09 ± 0.02	0.32 ± 0.06	0.64 ± 0.13	0.47 ± 0.07	0.37 ± 0.07	0.48 ± 0.07	0.40 ± 0.08
^{129}Sb	γ		0.20 ± 0.05	0.34 ± 0.05	0.90 ± 0.13	0.61 ± 0.09	0.58 ± 0.10	0.51 ± 0.07	0.62 ± 0.11
^{131}I	γ	1.40 ± 0.07	1.87 ± 0.08	2.13 ± 0.08	2.75 ± 0.16	2.01 ± 0.09	1.67 ± 0.10	1.76 ± 0.08	1.69 ± 0.09
^{132}Te (I)	γ	2.74 ± 0.08	3.25 ± 0.09	3.42 ± 0.10	3.80 ± 0.13	2.98 ± 0.15	2.72 ± 0.11	2.78 ± 0.11	2.77 ± 0.09
^{133}I	γ	4.11 ± 0.15	4.85 ± 0.15	5.19 ± 0.17	5.64 ± 0.19	4.51 ± 0.15	4.23 ± 0.14	4.34 ± 0.14	4.32 ± 0.12
^{134}Te	γ	6.97 ± 0.44	7.44 ± 0.76	7.68 ± 0.61	8.08 ± 0.53	6.33 ± 0.40	6.62 ± 0.41	6.80 ± 0.51	7.16 ± 0.32
^{135}I	γ	5.92 ± 0.18	6.18 ± 0.17	6.12 ± 0.17	5.98 ± 0.19	5.38 ± 0.16	5.42 ± 0.16	5.49 ± 0.16	5.58 ± 0.15
^{138}Cs	γ	6.36 ± 0.31	6.29 ± 0.27	6.18 ± 0.35	5.93 ± 0.28	6.04 ± 0.36	6.15 ± 0.37	5.85 ± 0.33	5.95 ± 0.34
^{139}Ba	γ	8.34 ± 0.64	7.56 ± 0.62	7.56 ± 0.60	7.24 ± 0.88	7.05 ± 0.69	8.16 ± 0.77	7.49 ± 0.63	6.61 ± 0.71
^{140}Ba (La)	γ	8.95 ± 0.25	8.60 ± 0.23	8.01 ± 0.20	7.75 ± 0.55	8.08 ± 0.23	8.70 ± 0.34	8.38 ± 0.23	7.87 ± 0.35
^{141}Ba, Ce	γ	8.90 ± 0.45	7.69 ± 0.41	8.14 ± 0.41	7.37 ± 0.55	8.41 ± 0.63	8.00 ± 0.83	7.64 ± 0.61	7.27 ± 0.57
^{142}La	γ	7.23 ± 0.38	6.61 ± 0.39	6.27 ± 0.36	5.76 ± 0.43	6.51 ± 0.42	7.55 ± 0.94	7.01 ± 0.43	6.84 ± 0.36
^{143}Ce	γ	6.79 ± 0.38	6.45 ± 0.37	5.97 ± 0.35	5.59 ± 0.35	6.66 ± 0.40	7.67 ± 0.46	6.95 ± 0.41	6.94 ± 0.33
^{146}Ce	γ	4.45 ± 0.65	3.71 ± 0.70	3.33 ± 0.43	3.07 ± 1.11	3.67 ± 0.62	3.11 ± 0.50	3.13 ± 0.46	3.88 ± 0.49
^{147}Nd	γ	3.40 ± 0.97	3.32 ± 0.49	2.64 ± 0.34		3.02 ± 0.64		3.11 ± 0.57	2.88 ± 0.32
^{149}Nd	γ	1.38 ± 0.21	1.06 ± 0.16	1.10 ± 0.15	1.45 ± 0.35	1.17 ± 0.30	1.29 ± 0.22	1.02 ± 0.22	1.08 ± 0.17

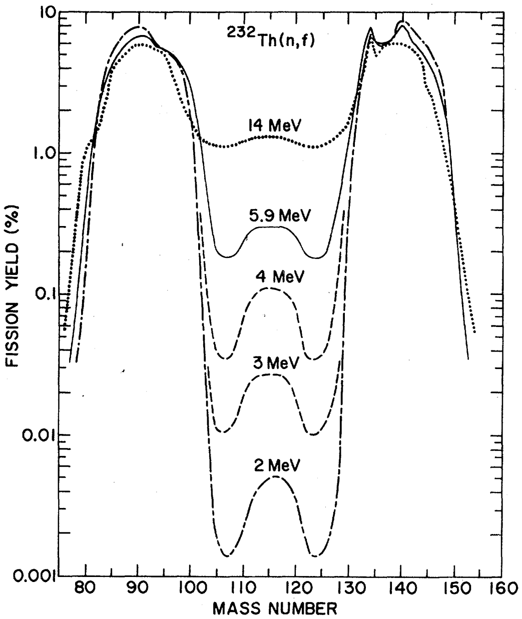

FIG. 1. Mass-yield curves for monoenergetic-neutron-induced fission of ^{232}Th.

from the fission yield data for monoenergetic-neutron-induced fission of ^{232}Th are presented in Table III. The mean mass (first moment) of the light fission product group is seen to remain essentially constant over the E_n range of 2–8 MeV, while the mean mass of the heavy group decreases by ~1 u, indicating that the increase in neutron emission per fission $\bar{\nu}$ with increasing excitation

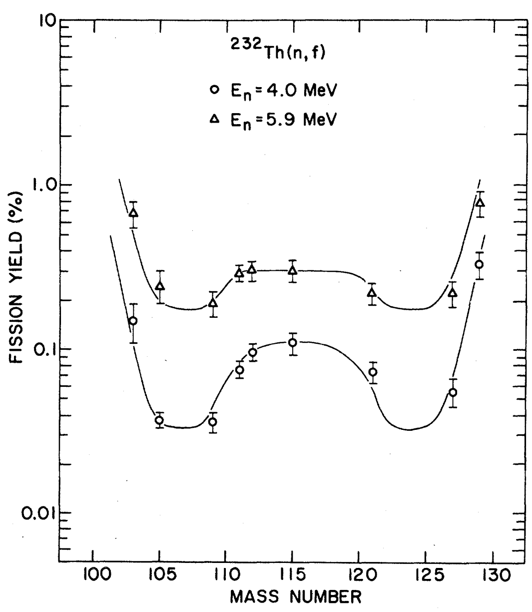

FIG. 2. Valley mass yields for ^{232}Th(n,f) showing third peak at symmetry.

energy is primarily from the heavy fragment. Values of $\bar{\nu}$ calculated from the mean masses are in reasonable agreement with experimental values based on direct measurement by fission-coincident neutron counting.[16]

Yield values for several valley fission products from the present work, combined with data from the literature, are plotted as a function of E_n in Fig. 3. Our data show clearly the effects of excitation energy on near-symmetric fission yields, i.e., the very sensitive increase in yield with increasing neutron energy, and distinct dips following the onset of second-chance fission (near E_n = 6 MeV), for which excitation energy is lowered by competition with neutron emission prior to fission. The latter effect was first seen by Bowles *et al.*[17] in proton-induced fission of ^{232}Th.

In contrast with the valley region, the yields of fission products in the asymmetric peaks of the mass distribution are not strongly dependent on incident neutron energy, but the effect of second-chance fission is nevertheless clearly apparent in the yield data plotted for several complementary asymmetric masses in Fig. 4. Distinct breaks in the yield vs E_n curves are seen for several masses in both the light and heavy peak regions.

Compared in Fig. 5 are the fission yields of a peak (^{143}Ce) and a valley (^{115}Cd) product as a function of E_n for ^{232}Th(n,f) and ^{238}U(n,f). Data for ^{238}U are taken from our previous publication.[7] Also shown (at the bottom of the figure) are the cross section curves for neutron-induced fission. Arrows indicate the approximate positions where second-chance fission (n,nf) becomes energetically possible. The more sensitive increase of valley yield with increasing E_n and the more pronounced effect of the onset of second-chance fission for ^{232}Th are clearly visible.

TABLE III. ^{232}Th(n,f) mass distribution characteristics.

E_n	Peak-to-valley ratio	Mean mass (u) Light group	Heavy group	$\bar{\nu}$ [a]	$\bar{\nu}$ [b]
2.0	1600	90.9	139.8	2.3	2.20
3.0	300	91.2	139.4	2.4	2.35
4.0	70	91.3	139.1	2.6	2.50
5.9	25	91.9	138.4	2.7	2.78
6.4	30	91.1	138.9	3.0	2.86
6.9	35	90.5	139.1	3.4	2.94
7.6	25	90.8	138.9	3.3	3.04
8.0	20	90.9	138.8	3.3	3.10
14.7	5	93.3	135.8	3.9	4.11

[a] Calculated from conservation of mass.
[b] Evaluated from experimental measurements by fission-coincident neutron counting (Ref. 16).

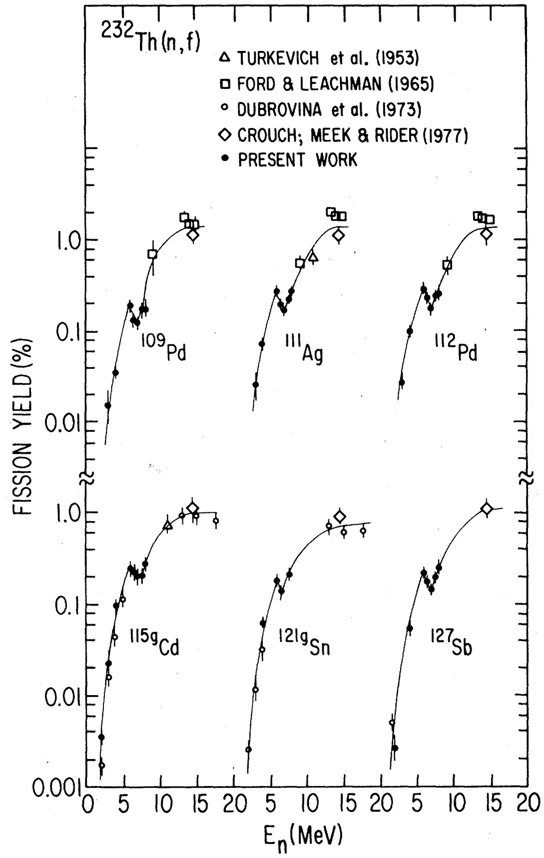

FIG. 3. Valley fission yields as a function of neutron energy for monoenergetic-neutron-induced fission of ^{232}Th.

The reason for the abrupt changes in the ^{232}Th (n,f) yields at the onset of second-chance fission and the relatively small changes in the ^{238}U(n,f)

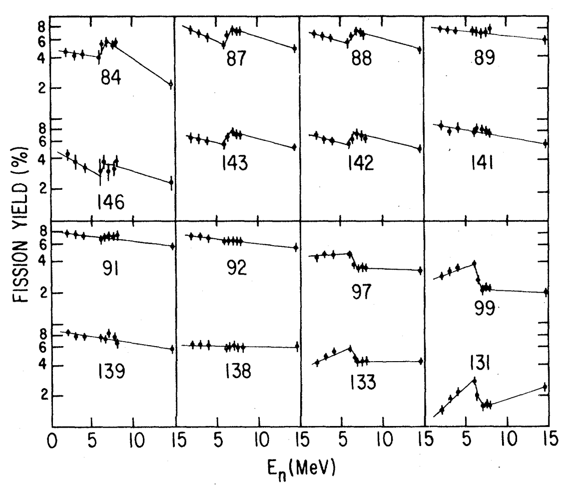

FIG. 4. Peak fission yields as a function of neutron energy for monoenergetic-neutron-induced fission of ^{232}Th.

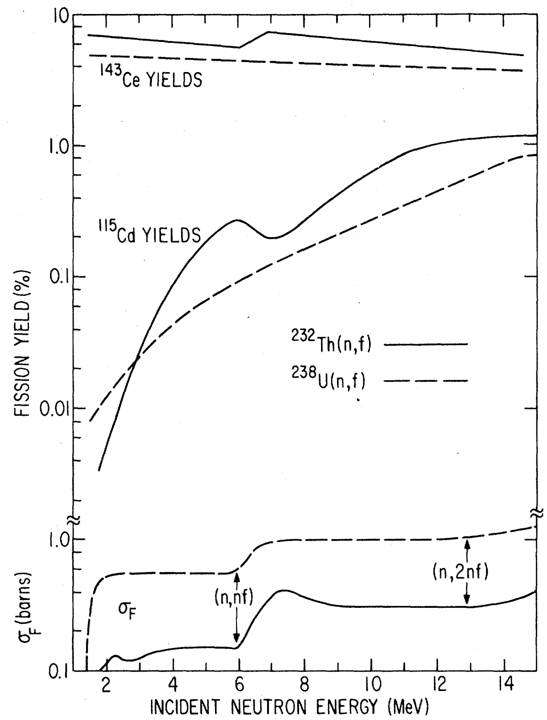

FIG. 5. Comparison of peak and valley yields and fission cross sections as a function of neutron energy for monoenergetic-neutron-induced fission of ^{232}Th and ^{238}U.

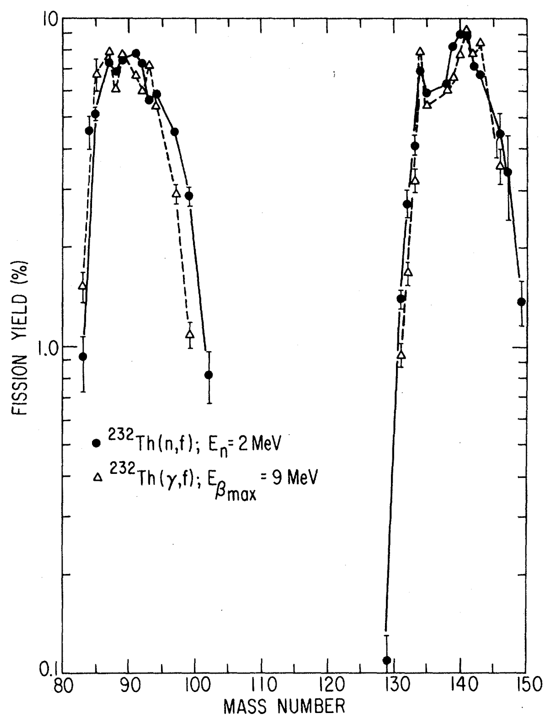

FIG. 6. Comparison of mass distributions for ^{232}Th(n,f) and ^{232}Th(γ,f).

TABLE IV. Calculated and measured ^{115}Cd yields for 6.9-MeV neutron-induced fission of ^{232}Th and ^{238}U.

Fissioning system	$\frac{\sigma_{f1}}{\sigma_f}$ [a]	$Y_1(E_n)$ [b] (%)	$\frac{\sigma_{f2}}{\sigma_f}$ [c]	$Y_2(E_n-\epsilon_n)$ [d] (%)	$Y(E_n)$ (%) calc	$Y(E_n)$ (%) exp
$^{232}Th(n,f)$	0.38	0.50	0.62	0.011	0.20	0.20 ± 0.03
$^{238}U(n,f)$	0.61	0.15	0.39	0.009	0.101	0.116 ± 0.012 [e]

[a] σ_{f1} determined by extrapolating σ_f from the region of first-chance fission.
[b] Y_1 determined by extrapolating the fission yields from the region of first-chance fission.
[c] $\sigma_{f2}=\sigma_f-\sigma_{f1}$, where σ_f is the fission cross section at $E_n=6.9$ MeV.
[d] $E_n-\epsilon_n=2.5$ MeV for $^{232}Th(n,f)$ and 1.5 MeV for $^{238}U(n,f)$.
[e] Data from Ref. 7.

yields is associated with the slopes of the yield vs E_n curves for the two fissioning systems. Once second-chance fission becomes energetically possible, the observed yield Y at energy E_n is given by the equation

$$Y(E_n)=\frac{\sigma_{f1}}{\sigma_f}Y_1(E_n)+\frac{\sigma_{f2}}{\sigma_f}Y_2(E_n-\epsilon_n)\,. \qquad (2)$$

The relative amounts of first- and second-chance fission yields are given by the ratios of first- and second-chance fission cross sections to the total fission cross section at E_n. The first-chance fission yield is evaluated at E_n, and the second-chance fission yield is evaluated at $E_n-\epsilon_n$, where ϵ_n is the amount of energy removed from the excited compound nucleus ^{233}Th or ^{239}U, by the emission of a neutron, and correction is made for the difference in fission thresholds between the first- and second-chance fissioning nuclei. If it is assumed that the yields of the second-chance fissioning nuclei ^{232}Th or ^{238}U behave in the same manner with E_n as the yields of the compound fissioning nuclei, then $Y_2(E_n-\epsilon_n)$ for ^{232}Th is reduced relatively much more for a valley fission product than is the yield for ^{238}U. Examples of the calculated ^{115}Cd yields for $^{232}Th(n,f)$ and $^{238}U(n,f)$ with 6.9 MeV neutrons are given in Table IV. This type of analysis accounts well for the yields of fission products found in the heavy-mass groups for both $^{232}Th(n,f)$ and $^{238}U(n,f)$, but not too well for the yields of fission products found in the light-mass groups. The reason for this is that the yields of the heavy-mass fission products for ^{232}Th or ^{238}U fission do not change appreciably from those for ^{233}Th or ^{239}U fission, provided the excitation energy above the fission thresholds is the same for either ^{232}Th and ^{233}Th or ^{238}U and ^{239}U. However, there is a shift of yields in the light-mass groups such that the average mass of this group is ~1 u less for ^{232}Th than for ^{233}Th. A similar phenomenon is observed for ^{238}U and ^{239}U.

The shift in yield with fissioning mass in the light-mass group and the relative constancy of the heavy-mass group is illustrated in Fig. 6 in which the mass distributions for 2 MeV neutron-induced fission and 9 MeV photofission of ^{232}Th are plotted. Photofission data are taken from the paper by Hogan *et al.*[18] The ^{233}Th compound nuclei are excited to ~7 MeV.[19] The ^{232}Th nuclei that undergo photofission have initial excitation energies from the fission threshold to 9 MeV. However, because of the enhanced photofission cross section at 6 MeV, most fission events occur in nuclei excited to this energy.[18] Thus the initial excitation energies of the fissioning ^{233}Th and ^{232}Th nuclei are comparable to within ~1 MeV. The difference in excitation energies may account for some of the observed increase in ^{233}Th fission yield for the heavy side of the light-mass group and the light side of the heavy-mass group. Other similarities in the two mass distribution are the fine-structure peaks at masses 134 and 140–141, but the fine-structure peak at mass 93 reported for $^{232}Th\ (\gamma,f)$ (Ref. 18) is not observed in $^{232}Th(n,f)$.

This work was performed under the auspices of the Office of Basic Energy Sciences, Division of Nuclear Science, U. S. Department of Energy.

[1]G. P. Ford and R. B. Leachman, Phys. Rev. 137, 826 (1965).
[2]S. M. Dubrovina, V. I. Novgorodtseva, L. N. Morozov, V. A. Pchelin, L. V. Christyakov, V. A. Shigin, and V. M. Shubko, Yad. Fiz. 17, 470 (1973) [Sov. J. Nucl. Phys. 17, 240 (1973)].
[3]E. A. C. Crouch, At. Data Nucl. Data Tables 19, 419 (1977).
[4]M. E. Meek and B. F. Rider, General Electric Vallecitos Nuclear Center Report No. NEDO-12154-2, 1977 (unpublished).
[5]S. A. Cox and P. R. Hanley, IEEE Trans. Nucl. Sci. 18,

108 (1971).
[6]D. L. Smith and J. W. Meadows, Nucl. Sci. Eng. 58, 314 (1975).
[7]S. Nagy, K. F. Flynn, J. E. Gindler, J. W. Meadows, and L. E. Glendenin, Phys. Rev. C 17, 163 (1978).
[8]K. F. Flynn, Argonne National Laboratory Report No. ANL-75-24, 1975 (unpublished).
[9]J. B. Cummins, National Academy of Science-National Research Council Publication No. NAS-NS-3107, 1962 (unpublished), p. 25.
[10]R. Gunnink and J. B. Niday, Lawrence Livermore Laboratory Report No. UCRL-51061, 1972 (unpublished).
[11]J. Blachot and C. Fiche, At. Data Nucl. Data Tables 20, 241 (1977).
[12]M. J. Martin, editor, Oak Ridge National Laboratory Report No. ORNL-5114, 1976 (unpublished); D. C. Kocher, Oak Ridge National Laboratory Report No. ORNL/NUREG/TM-102, 1977 (unpublished).
[13]K. Wolfsberg, Los Alamos Scientific Laboratory Report No. LA-5553-MS, 1974 (unpublished).
[14]S. Amiel and H. Feldstein, Phys. Rev. C 11, 845 (1975).
[15]B. R. Erdal, J. C. Williams, and A. C. Wahl, J. Inorg. Nucl. Chem. 31, 2993 (1969).
[16]F. Manero and V. A. Konshin, At. Energy Rev. 10, 637 (1972).
[17]B. J. Bowles, F. Brown, and J. P. Butler, Phys. Rev. 107, 751 (1957).
[18]J. C. Hogan, A. E. Richardson, J. L. Meason, and H. L. Wright, Phys. Rev. C 16, 2296 (1977).
[19]W. O. Meyers and W. J. Swiatecki, Lawrence Radiation Laboratory Report No. UCRL-11980, 1965 (unpublished).